

Interferometric synthetic aperture radar atmospheric correction: Medium Resolution Imaging Spectrometer and Advanced Synthetic Aperture Radar integration

Zhenhong Li,¹ Eric J. Fielding,² Paul Cross,¹ and Jan-Peter Muller¹

Received 22 November 2005; revised 8 February 2006; accepted 14 February 2006; published 25 March 2006.

[1] Atmospheric water vapor effects represent one of the major limitations of repeat-pass InSAR, and limit the accuracy of deformation rates derived from InSAR. The use of contemporaneous MERIS data to correct ENVISAT ASAR measurements shows a significant reduction in water vapor effects. After correction, the RMS differences between GPS and InSAR range changes in the satellite line of sight direction decreased to 0.55 cm with a reduction of up to 0.35 cm. It is also shown that it is possible to implement an extra ‘conservative’ cloud mask and obtain better water vapor corrections than that from using the official ESA cloud mask product. **Citation:** Li, Z., E. J. Fielding, P. Cross, and J.-P. Muller (2006), Interferometric synthetic aperture radar atmospheric correction: Medium Resolution Imaging Spectrometer and Advanced Synthetic Aperture Radar integration, *Geophys. Res. Lett.*, *33*, L06816, doi:10.1029/2005GL025299.

1. Introduction

[2] Spaceborne repeat-pass Synthetic Aperture Radar Interferometry (InSAR) provides a powerful tool to detect surface displacement with sub-centimeter accuracy and tens-of meters resolution. A major source of error for repeat-pass InSAR is the phase delay in radio signal propagation through the atmosphere, especially the part due to tropospheric water vapor. Zebker *et al.* [1997] suggested that a 20% spatial or temporal change in relative humidity could result in a 10–14 cm error in deformation measurement retrievals, independent of baseline parameters. Calibration techniques to spatially reduce path delays using continuous Global Positioning System (CGPS) and the NASA Moderate Resolution Imaging Spectroradiometer (MODIS) data have been well demonstrated [e.g., Williams *et al.*, 1998; Wadge *et al.*, 2002; Li *et al.*, 2005, 2006a]. A disadvantage of using GPS data to correct InSAR measurements is that it requires a dense GPS network, and this is impractical, especially in remote areas. On the other hand, a limitation of MODIS-based water vapor correction models is the time difference between MODIS and SAR acquisitions since the instruments are aboard different satellites [Li *et al.*, 2005].

[3] The Medium Resolution Imaging Spectrometer (MERIS) was launched together with the Advanced

Synthetic Aperture Radar (ASAR) on the European Space Agency (ESA) ENVISAT spacecraft on 1 March 2002. MERIS is a push-broom passive imaging instrument and measures the solar radiation reflected from the Earth’s surface and clouds in the visible and near IR spectral range during the daytime with a swath width of 1150 km for the total 68.5° field of view [European Space Agency, 2002] (accessed 12 Jan 2006). MERIS has two out of fifteen narrow spectral channels in the near-IR for the remote sensing of Precipitable Water Vapor (PWV) either above land or ocean surfaces under cloud free conditions [Bennartz and Fischer, 2001] or above the highest cloud level under cloudy conditions [Albert *et al.*, 2001]. MERIS near-IR PWV products are available at two spatial resolutions. In full resolution (FR) mode each pixel has an instantaneous field of view of 0.019°, with a nadir spatial sampling of 260 m across track by 290 m along track. In reduced resolution (RR) mode each nadir pixel is approximately 1.04 km across track by 1.2 km along track.

[4] Although MERIS and ASAR are operated independently, these two data sets can be acquired simultaneously during the daytime, and ASAR IS1 to IS5 mode and most of the Wide Swath mode coverage falls within the MERIS coverage (<http://www.eurimage.com/products/envisat.html>), so MERIS PWV data can be available to correct most daytime ASAR measurements. Li *et al.* [2006b] have reported that: (1) the agreement between MERIS and GPS/radiosonde PWV was about 1.1 mm (1.0mm of PWV ~ 6.2mm of Zenith Wet Delays (ZWD)) in terms of standard deviations; and (2) Since MERIS PWV is sensitive to the presence of clouds, the low frequency of global cloud free conditions (~25%) can be a major limitation in applying MERIS data to InSAR atmospheric correction. However, it has been shown that the frequency can, for some areas, be much higher, for example, 38% for Eastern Tibet and 48% for Southern California. This suggests that MERIS near-IR PWV products show potential for correcting ASAR measurements in certain regions [Li *et al.*, 2006b], which is investigated in this study.

2. Data Processing Strategy

2.1. MERIS-Derived Zenith Path Delay Difference Maps (ZPDDM)

[5] For InSAR atmospheric correction, Zenith Path Delay Difference Maps (ZPDDM) can be derived from MERIS data as follows: In step 1, MERIS-PWV needs to be converted into ZWD using surface temperature measurements, which can be obtained from one or more meteorological stations including radiosondes and/or GPS [Li, 2005]; In step 2, a ZPDDM can be calculated by

¹Department of Geomatic Engineering, University College London, London, UK.

²Jet Propulsion Laboratory, California Institute of Technology, Pasadena, California, USA.

Table 1. Interferograms (Ifms) Used in This Study

	Region	Date 1	Date 2	Δt , days	B_{\perp} , m ^a	σ , rad ^b
Ifm1	SCIGN	07-Aug-2004	29-Jan-2005	175	-12 to -34	0.17
Ifm2	SCIGN	07-Aug-2004	09-Apr-2004	245	-29 to -92	0.45
Ifm3	Qum	22-Aug-2003	26-Sep-2003	35	-40 to -51	0.25

^aPerpendicular baseline at center of swath which varies along the track between the values shown.

^bPhase error due to the topographic uncertainty of SRTM DEM (7m) [Farr and Kobrick, 2000].

differencing two 2D ZWD fields; In step 3, since MERIS near-IR PWV is sensitive to the presence of clouds, there are often missing values in MERIS near-IR PWV fields due to clouds. An improved inverse distance weighted interpolation method (IIDW) [Li, 2004] can be applied to fill in the cloudy pixels using the cloud-free ZWD differences; In step 4, in common with the GPS/MODIS integrated model [Li *et al.*, 2005], to suppress the inherent noise of MERIS-PWV, a low-pass filter can be applied to the ZPDDM with an average width of c. 0.6 km for FR MERIS data and c. 2.4 km for RR MERIS data. Assuming pixel to pixel PWV errors are uncorrelated, the accuracy of the ZPDDM increases by a factor of 2 at the expense of spatial resolution. Note that Step 3 can be inserted before Step 2 if there are only a few pixels with missing values due to ‘wispy’ clouds. Application of the IIDW to ZWD differences instead of the ZWD values before differencing is often helpful to reduce topographic effects on the water vapor variation [Li *et al.*, 2006a].

2.2. Interferometric Processing Strategy

[6] Two pairs of ESA ENVISAT ASAR images on track 170 (descending: satellite moving south) over the Southern California Integrated GPS Network (SCIGN) region, along with one pair on track 149 (descending) over Qum, Iran, were used to investigate the MERIS water vapor correction model in this study (Table 1). The interferograms were processed from ASAR level 0 (raw data) products using the ROI_PAC software (version 2.3) [Rosen *et al.*, 2004]. To reduce water vapor effects on the interferograms, ZPDDM needs to be inserted into the interferometric processing sequence after removal of topographic signals by use of a precise DEM [Li *et al.*, 2005, 2006a]. See the auxiliary material¹ for more details.

3. Applications of MERIS Water Vapor Correction Models

3.1. The SCIGN Region

[7] The Los Angeles region exhibits large seasonal horizontal and vertical movements (e.g., up to 14 mm and 110 mm respectively over the period from 1997 to 1999) [Bawden *et al.*, 2001]. In order to validate the MERIS correction model over the SCIGN region, independent 3D GPS-derived displacements provided by the Scripps Orbit and Permanent Array Center (SOPAC) [Nikolaidis, 2002] were compared with InSAR results in the satellite line of sight (LOS) direction.

[8] Figures 1a and 1b show the interferogram (Ifm1) spanning 175 days from 7 August 2004 to 29 January 2005, before and after correction respectively. Phase varia-

tion of the unwrapped phase decreased from 2.38 rad before correction to 1.49 rad after correction, implying that the unwrapped phase becomes much flatter. Comparisons between GPS and InSAR range changes in the LOS showed that the RMS difference decreased from 0.89 cm before correction to 0.54 cm after correction (Figure S1), which indicates that the application of this MERIS correction model improved this interferogram.

[9] In Figure 1, black solid triangles represent GPS stations where the differences between InSAR and GPS range changes are within *or* beyond a 1-sigma range both before and after correction; white squares with black borders represent GPS stations only when differences are greater than 1-sigma before correction, *but* within a 1-sigma range after correction (i.e., white squares with black borders imply improvement after correction); red solid circles represent GPS stations only when differences are within a 1-sigma range before correction, *but* greater than 1-sigma after correction (i.e., red solid circles indicate deterioration after correction). In Figure 1, there are 70 GPS stations in total, 26 (i.e., 37%) white squares and only 3 (i.e., 4%) red solid circles, confirming that the MERIS correction model drastically reduced water vapor effects. It should be noted that all 3 red solid circles are located in mountainous areas with steep slopes. One possible cause for this is that the accuracy of MERIS near-IR PWV products degrades due to shadows cast by steep slopes (P. Albert, personal communication, 2006). Another possibility is the difficulty in identifying cloudy pixels in mountainous areas due to strong variations in ground conditions (slope and cover

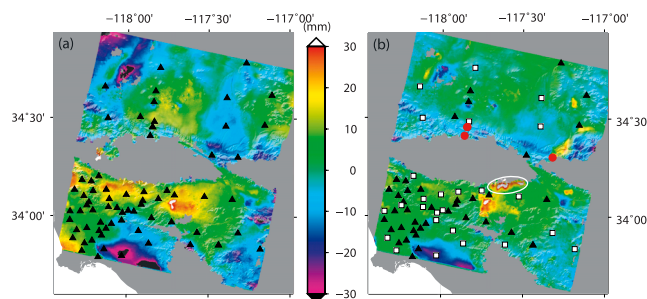


Figure 1. Ifm1 (040807-050129) superimposed on a SRTM DEM. (a) Original Ifm; (b) Corrected Ifm using MERIS data. Grey within Ifm1 coverage implies areas with low coherence due to steep slopes and vegetation. Negative values imply that the surface moves towards the satellite; that is, the pixel exhibits uplift in the LOS. In Figure 1b black solid triangles, white squares and red solid circles represent GPS stations with little change, improvement and deterioration respectively, after correction. The white oval in Figure 1b is believed to be due to MERIS data. See more in text.

¹Auxiliary material is available at <ftp://ftp.agu.org/apend/gl/2005gl025299>.

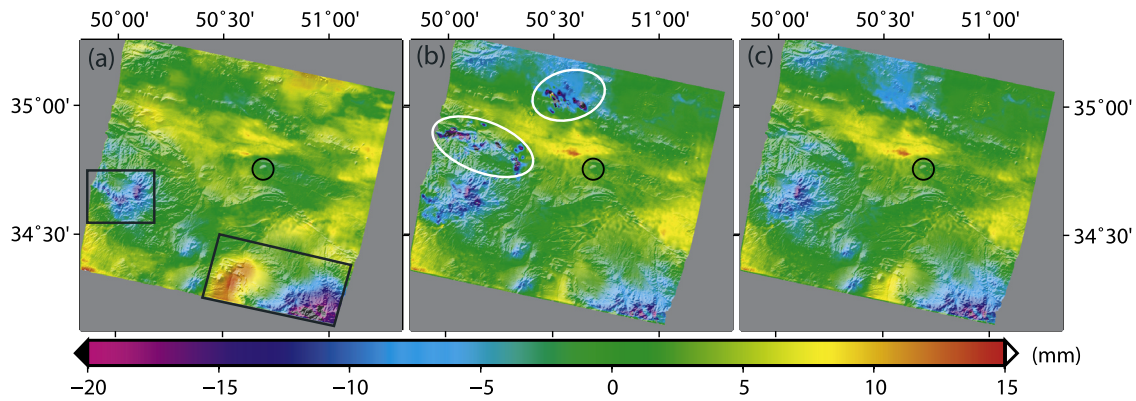


Figure 2. Ifm3 (030822-030926) superimposed on a SRTM DEM. (a) Original Ifm where black rectangles represent areas affected by water vapor. (b) Corrected Ifm using MERIS data with the official ESA cloud mask product. The white ovals represent errors due to the failure to identify clouds in the MERIS PWV field collected on 22 August 2003. (c) Corrected Ifm using MERIS data with ‘conservative’ cloud mask product, see text. Note the black circle represents Qum Kuh.

including snow or ice in some places) within the MERIS pixels. A visual inspection of cloud images showed that the artifact indicated by a white oval in Figure 1 was coincident with the presence of clouds on 29 January 2005, suggesting that this feature was due to the errors in MERIS cloud mask data. These suggest that caution needs to be exercised when interpreting the results of the MERIS water vapor correction model, particularly over mountainous areas.

[10] Ifm2, spanning 245 days from 7 August 2004 to 9 April 2005, is shown in Figure S2. Phase variation decreased from 1.73 rad before correction to 1.22 rad after correction, and the RMS difference between GPS and InSAR decreased from 0.83 cm to 0.59 cm (Figure S2c). 23 out of 63 stations (i.e., 37%) are white squares, whilst 2 out of 63 (3%) are red solid circles. It should be noted that the 2 red solid circles are also observed at stations with slopes.

3.2. Qum, Iran

[11] Since MERIS near-IR PWV is sensitive to the presence of clouds, the accuracy of the cloud mask product used to identify cloudy pixels is vital. In order to investigate the impact of an ‘imperfect’ cloud mask product on the MERIS correction model, an ASAR interferogram (Ifm3,

Table 1) spanning 35 days over Qum, Iran was analyzed (Figure 2). Qum was selected as a test site because of its arid climate and high frequency of cloud-free conditions.

[12] In Figure 2, the black circle marks the small but mature salt fountain of Kuh-e-namak (mountain of salt in Farsi) near the city of Qum (hereafter abbreviated to Qum Kuh). It is reported that the salt of Qum Kuh extrudes from a diapir along a strike-slip fault at up to 82 mm/y [Talbot and Aftabi, 2004]. The displacement of Qum Kuh during a period of 35 days should be less than 8 mm, which is slightly greater than the phase variation of Ifm3 before correction, 4.5 mm (1.00 rad) (Figure 2a). However, the displacement can be considered negligible because it is such a small area.

[13] It is clear that the signals within the black rectangles in Figure 2a are highly correlated with topography, and these signals were significantly reduced after correction (Figure 2a versus 2b), implying that these signals are due to topography-dependent water vapor effects. In Figure 2b, additional signals can be observed after correction (indicated by white ovals). On closer inspection of the MERIS PWV fields, it was found that these signals were coincident with low PWV values (also indicated by white ovals) appearing in the MERIS PWV field collected on

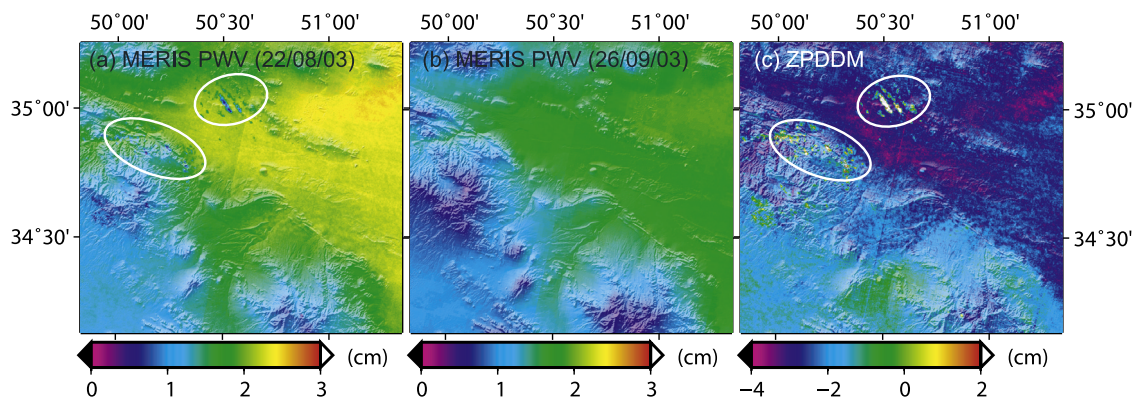


Figure 3. (a) MERIS PWV field collected on 22 August 2003. (b) MERIS PWV field collected on 26 September 2003. (c) ZPDDM $\approx 6.2 \times (\text{PWV}^b - \text{PWV}^a)$. Note the white ovals represent errors due to the failure to identify clouds in the MERIS PWV field collected on 22 August 2003.

22 August 2003 (Figure 3a), suggesting that these features are a result of the uncertainties of in the MERIS data of 22 August 2003. Note that Terra MODIS data was collected 72 minutes after the MERIS data (Figure S3b), and the MODIS cloud mask indicated the presence of clouds over the areas of interest (indicated by white ovals). Where light is backscattered from the tops of clouds, MERIS will measure lower PWV values. This suggests that the additional signals are likely to be due to the fact that cloudy pixels were falsely identified as cloud free in the official ESA MERIS cloud mask.

[14] Photons in the oxygen absorption band, used to determine surface pressure, see the same scattering and surface properties as photons in the water vapor absorption band. Therefore, surface pressure can be used to detect thin clouds (cirrus) [Ramon *et al.*, 2002; R. Preusker, personal communication, 2005]. In this study, we adopted the following ‘conservative’ cloud flag to identify cloud-free pixels: (1) the ESA cloud mask should indicate clear, and; (2) the difference between the MERIS-derived surface pressure and the estimated surface pressure from the mean sea level pressure (from ECMWF and recorded in the MERIS product) adjusted to local elevation should not exceed a given threshold. Using this mask, the 22/08/2003 MERIS PWV field was used to produce a ZPDDM to correct the ASAR measurements. Comparing Figures 2b and 2c, it is clear that the water vapor signals were significantly reduced, suggesting that implementing an extra ‘conservative’ cloud mask can provide better water vapor corrections than using the ESA standard product.

4. Discussion and Conclusions

[15] This paper has demonstrated the successful application of a MERIS water vapor correction model to ENVISAT ASAR data for the first time. After correction, the RMS differences between GPS and InSAR range changes decreased to 0.55 cm with a reduction of up to 0.35 cm. There are several advantages of the MERIS correction model over GPS and MODIS based correction models: (1) the high spatial resolution (to 300 m) of MERIS data, (2) MERIS and ASAR data are collected simultaneously, and (3) MERIS and ASAR have a virtually identical propagation path. Some caution needs to be exercised when interpreting the results of the MERIS correction model, particularly over mountainous areas. A simple criterion to discriminate a real geophysical signal from an artifact due to uncertainties in the MERIS PWV products is to determine whether a signal is coincident with the presence of clouds. If this is the case, then the signal is likely to be due to errors in the MERIS data. A pair-logic method or an independent water vapor correction (e.g., MODIS) can also be used to identify water vapor errors introduced by the MERIS products.

[16] This study successfully demonstrates that a ‘conservative’ cloud mask can detect and mask out thin clouds to obtain better water vapor corrections than those obtained using the ESA standard product. The topic of deriving cloud masks for MERIS PWV product does, however, still need further research.

[17] **Acknowledgments.** This work has been carried out within the NERC Earth Observation Centre of Excellence: COMET. Part of this research was carried out at JPL/Caltech under contract with NASA. We are grateful to two anonymous reviewers and Eric Calais for thoughtful and thorough reviews, and to R. Preusker, P. Albert and A. Sibthorpe for useful discussions. We thank JPL/Caltech for the use of the ROI_PAC software to generate our interferograms [Rosen *et al.*, 2004]. The ASAR and MERIS data were supplied under ESA ENVISAT data grants AOE.668, AOE.853 and C1P.3336, and the GPS data were obtained from the Scripps Orbit and Permanent Array Centre (SOPAC, <http://sopac.ucsd.edu>).

References

- Albert, P., R. Bennartz, and J. Fischer (2001), Remote sensing of atmospheric water vapor from backscattered sunlight in cloudy atmospheres, *J. Atmos. Oceanic Technol.*, *18*, 865–874.
- Bawden, G. W., W. Thatcher, R. S. Stein, K. W. Hudnut, and G. Peltzer (2001), Tectonic contraction across Los Angeles after removal of ground-water pumping effects, *Nature*, *412*, 812–815.
- Bennartz, R., and J. Fischer (2001), Retrieval of columnar water vapour over land from back-scattered solar radiation using the Medium Resolution Imaging Spectrometer (MERIS), *Remote Sens. Environ.*, *78*, 271–280.
- European Space Agency (2002), *MERIS Product Handbook*, Issue 1.3, Paris. (Available at: <http://envisat.esa.int/dataproducts/meris>)
- Farr, T. G., and M. Kobrick (2000), Shuttle Radar Topography Mission produces a wealth of data, *Eos Trans. AGU*, *81*(48), 583–585.
- Li, Z. (2005), Correction of atmospheric water vapour effects on repeat-pass SAR interferometry using GPS, MODIS and MERIS data, Ph.D. thesis, University College London, London.
- Li, Z. (2004), Production of regional 1 km × 1 km water vapor fields through the integration of GPS and MODIS data, paper presented at Global Navigation Satellite System Technical Meeting 2004, Inst. of Navig., Long Beach, Calif.
- Li, Z., J. Muller, P. Cross, and E. J. Fielding (2005), Interferometric synthetic aperture radar (InSAR) atmospheric correction: GPS, Moderate Resolution Imaging Spectroradiometer (MODIS), and InSAR integration, *J. Geophys. Res.*, *110*, B03410, doi:10.1029/2004JB003446.
- Li, Z., E. J. Fielding, P. Cross, and J. Muller (2006a), Interferometric synthetic aperture radar atmospheric correction: GPS topography-dependent turbulence model, *J. Geophys. Res.*, *111*, B02404, doi:10.1029/2005JB003711.
- Li, Z., J.-P. Muller, P. Cross, P. Albert, J. Fischer, and R. Bennartz (2006b), Assessment of the potential of MERIS near-infrared water vapour products to correct ASAR interferometric measurements, *Int. J. Remote Sens.*, *27*, 349–365, doi:10.1080/01431160500307342.
- Nikolaidis, R. (2002), Observation of geodetic and seismic deformation with the Global Positioning System, Ph.D. thesis, Univ. of Calif., San Diego, La Jolla.
- Ramon, D., R. Santer, and P. Dubuisson (2002), MERIS surface pressure and cloud flag: Present status and improvements, paper presented at Envisat Validation Workshop, Eur. Space Res. Inst., Frascati, Italy.
- Rosen, P. A., S. Hensley, G. Peltzer, and M. Simons (2004), Updated Repeat Orbit Interferometry package released, *Eos Trans. AGU*, *85*(5), 47.
- Talbot, C., and P. Aftabi (2004), Geology and models of salt extrusion at Qum Kuh, central Iran, *J. Geol. Soc. London*, *161*, 321–334.
- Wadge, G., et al. (2002), Atmospheric models, GPS and InSAR measurements of the tropospheric water vapour field over Mount Etna, *Geophys. Res. Lett.*, *29*(19), 1905, doi:10.1029/2002GL015159.
- Williams, S., Y. Bock, and P. Fang (1998), Integrated satellite interferometry: Tropospheric noise, GPS estimates and implications for interferometric synthetic aperture radar products, *J. Geophys. Res.*, *103*, 27,051–27,068.
- Zebker, H. A., P. A. Rosen, and S. Hensley (1997), Atmospheric effects in interferometric synthetic aperture radar surface deformation and topographic maps, *J. Geophys. Res.*, *102*, 7547–7564.

P. Cross, Z. Li, and J.-P. Muller, Department of Geomatic Engineering, University College London, Gower Street, London WC1E 6BT, UK. (zgli@ge.ucl.ac.uk)

E. J. Fielding, Jet Propulsion Laboratory, California Institute of Technology, 4800 Oak Grove Drive, Pasadena, CA 91109, USA.